

NANO EXPRESS

Open Access



Core-shell of FePt@SiO₂-Au magnetic nanoparticles for rapid SERS detection

Andri Hardiansyah¹, An-Yu Chen¹, Hung-Liang Liao¹, Ming-Chien Yang^{1*}, Ting-Yu Liu^{2*}, Tzu-Yi Chan², Hui-Ming Tsou², Chih-Yu Kuo³, Juen-Kai Wang^{4,5} and Yuh-Lin Wang^{5,6}

Abstract

In this study, multifunctional hybrid nanoparticles composed of iron platinum (FePt), silica (SiO₂), and gold nanoparticles (AuNPs) had been developed for surface-enhanced Raman scattering (SERS) application. Core-shell structure of SiO₂ and FePt nanoparticles (FePt@SiO₂) was fabricated through sol-gel process and then immobilized gold nanoparticles onto the surface of FePt@SiO₂, which displays huge Raman enhancement effect and magnetic separation capability. The resulting core-shell nanoparticles were subject to evaluation by transmission electron microscopy (TEM), Energy-dispersive X-ray spectroscopy (EDX), zeta potential measurement, and X-ray photoelectron spectroscopy (XPS). TEM observation revealed that the particle size of resultant nanoparticles displayed spherical structure with the size ~30 nm and further proved the successful immobilization of Au onto the surface of FePt@SiO₂. Zeta potential measurement exhibited the successful reaction between FePt@SiO₂ and AuNPs. The rapid SERS detection and identification of small biomolecules (adenine) and microorganisms (gram-positive bacteria, *Staphylococcus aureus*) was conducted through Raman spectroscopy. In summary, the novel core-shell magnetic nanoparticles could be anticipated to apply in the rapid magnetic separation under the external magnetic field due to the core of the FePt superparamagnetic nanoparticles and label-free SERS bio-sensing of biomolecules and bacteria.

Keywords: Core-shell nanoparticles, Surface-enhanced Raman scattering, Magnetic separation, Bio-detection

Background

Rapid, specific, accurate, and sensitive identification and detection of small molecules and pathogenic bacteria are essential toward clinical treatment of infectious diseases. Traditional approaches for the pathogen bacteria identification often requires time-consuming bacteria culture and amplification protocols. Conventional protocols for microbial detection, though reliable and gold standard, are time and cost consuming and inconvenient for field situation [1, 2]. In this respect, sensitivity of bacteria into antibiotic depends mostly on measuring the change of its proliferation in response to the drug. Thus, in order to overcome these challenges, there is a development of new protocols and its combination with nanotechnology as a new method for the higher sensitivity and low-cost

strategies for fast bio-detection and identification of small molecules or bacteria [1, 3, 4].

Raman spectroscopy elaborates the molecular vibrational signal to be used to identify and detect the molecular species such as small molecules and bacteria. Surface-enhanced Raman scattering (SERS) technique has attracted a lot of attention for more than three decades [5–7] because it enhances the Raman signal of the small molecules and or bacteria by several orders of magnitude. SERS nanotechnology could observe the monolayer (single-molecule level) [8] and studies on the identification of biological species, i.e., three kinds species of microbes (gram-positive, gram-negative, and mycobacteria), which have been reported in our previous work [3, 5]. The enhancement is known to develop from the strong optical intensity localized between the surface of metallic nanostructure [8]. SERS takes advantage of localized surface plasmon resonance (LSPR) in nanoscale systems based on metallic nanoparticles such as silver and gold. The enhancements ranging from a factor of

* Correspondence: myang@mail.ntust.edu.tw; tylu0322@gmail.com

¹Department of Materials Science and Engineering, National Taiwan University of Science and Technology, Taipei 10607, Taiwan

²Department of Materials Engineering, Ming Chi University of Technology, New Taipei City 24301, Taiwan

Full list of author information is available at the end of the article

10^6 to 10^{16} have been reported in various studies [9–11]. The mechanisms for this enhancement in SERS are attributed to electromagnetic field enhancement due to localized surface plasmon resonance and also to chemical interactions of the analytic molecules with the substrate moiety. As a result of these enhancements, SERS can have the sensitivity for the identification of ultra-trace levels of analytes to single molecules and bacteria. This level of sensitivity is useful for the detection of a small number of analytic molecules normally found in a cellular compartment [12]. Recently, the development of SERS active particles have been successfully used as labels or probes in immunoassays, bacteria, and DNA detection [3, 13–18].

The incorporation of nanoparticles through self-assembly mechanism provides an interesting characteristic in nanotechnology application. Core-shell nanoparticles have emerged as an important type of functional nanostructures with promising applications in many fields, especially in health sciences and biomaterials applications. Nanoparticles have also been assembled and bound to functionalized moiety with various mechanisms [19].

Various nanostructures have been synthesized in diverse formulations and functionalization whether using a single or multiple nanoparticles. For instance, iron oxide nanoparticles have been used for cellular separation and contrast agent. Silver nanoparticles have been used for bactericidal and SERS detection agent. Gold nanoparticles have been used for imaging, photothermal therapy, and LSPR detection. The most common and well investigated metallic nanoparticles, gold nanoparticles hold particularly interesting characteristics. Gold nanoparticles were applied in the significant place in medicine, material sciences, as well as diagnostics for their unique optical and physiochemical properties [1, 20–25]. Their facile synthesis and bio-conjugation procedures, along with its unique surface plasmon properties, made gold nanoparticles practicable in labs without expensive or sophisticated equipment [26–28].

Moreover, gold nanoparticles have also been combined with various nanostructures in order to develop SERS substrate [27, 29]. In this work, the core-shell nanoparticles were developed by functionalized amino-silane around FePt nanoparticles (FePt@SiO₂) nanoparticles and then grafted the gold nanoparticles onto the surfaces of FePt@SiO₂ nanoparticles. Systematic characterizations have been conducted in order to elaborate the morphology and chemical properties of the hybrid nanoparticles. The coverage of the gold nanoparticles and clusters on the surfaces of the silica nanoparticles was evaluated using transmission electron microscopy (TEM). Zeta potential measurement was conducted to evaluate the surface charges of nanoparticles. Furthermore, SERS detection was conducted toward adenine and *Staphylococcus aureus* to

elaborate the Raman enhancement signals using the novel core-shell nanoparticles.

Methods

Materials

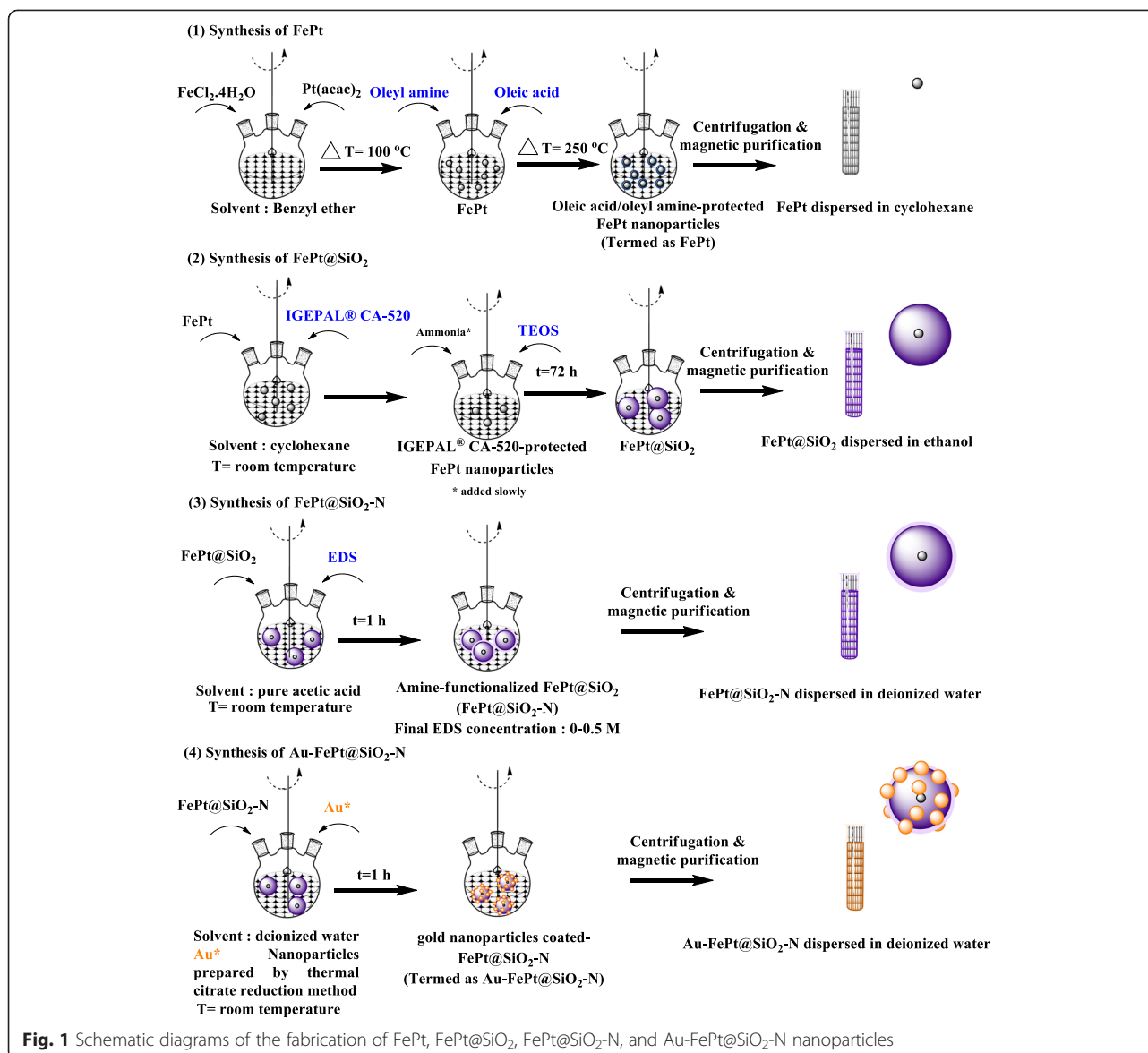
Iron (II) chloride tetrahydrate (FeCl₂·4H₂O) (>99 %), platinum (II) acetylacetonate, (Pt(acac)₂) (>99.9 %), oleylamine (*cis*-1-amino-9-octadecene (≥98 %), oleic acid (*cis*-9-octadecenoic acid (>99 %), benzyl ether, cyclohexane (99.5 %)), IGEPAL® CA-520 (octylphenoxy poly(ethyleneoxy) ethanol, branched), tetraethyl orthosilicate (TEOS) (99.99 %), ammonia (≥99 %), *N*-[3-(trimethoxysilyl) propyl] ethylenediamine (energy-dispersive X-ray spectroscopy (EDS)) (97 %), acetic acid (CH₃COOH, ≥99 %), trisodium citrate dihydrate (Na₃C₆H₅O₇·2H₂O, ≥99.5 %), hydrogen tetrachloroaurate (III) trihydrate (HAuCl₄·3H₂O, 99 %), and adenine (C₅H₅N₅, ≥99 %) were purchased from Sigma Aldrich, St. Louis, MO, USA. Ethyl alcohol (ethanol, analytical standard) was purchased from Fluka Analytical, USA. Agar Bacteriological was purchased from Oxoid. Luria-Bertani (LB Broth) was purchased from Difco™. High-purity water purified by a Milli Q Plus water purifier system (Milipore, USA), with a resistivity of 18.3 M Ω cm, was used in all experiments. All the chemicals were used without further purification.

Synthesis of Iron Platinum Nanoparticles

Iron platinum (FePt) nanoparticles were synthesized through standard airless procedures. Briefly, FeCl₂·4H₂O (396 mg) and platinum (II) acetylacetonate (Pt(acac)₂) (196 mg) were mixed in benzyl ether (30 mL) with vigorous stirring under nitrogen atmosphere for 20 min. Further, the solution was heated to 100 °C. After reaching 100 °C, oleic acid (170 μL) and oleylamine (160 μL) were mixed into the solution under vigorous stirring for 20 min. Further, the solution was heated to 250 °C for 30 min which resulted in black colored solution of FePt. The solution was allowed to cool to room temperature. Purification was carried out by washing several times with ethanol (FePt: ethanol = 1:4 v/v) then centrifuged 6000 rpm for 20 min. The as-synthesized FePt nanoparticles were separated magnetically using a strong neodymium magnet. Dark yellow supernatant was discarded. The precipitate was uniformly dispersed in cyclohexane (Fig. 1).

Preparation of FePt@SiO₂

FePt nanoparticles were encapsulated into the silica nanoparticles through sol-gel processes. Briefly, 10 mL of FePt nanoparticles (26.5 mg/mL) and 8 mL of IGEPAL® CA-520 were mixed with 170 mL cyclohexane under vigorous stirring. Afterwards, 1.3 mL ammonia (30 %) was added slowly to the mixture followed by adding 1 mL triethoxysilane (TEOS), and the reaction was mixed



under vigorously stirring for 72 h. After 72 h, the encapsulated particles were mixed with ethanol and centrifuged 4500 rpm for 30 min to remove the excess silica formed during the hydrolysis-condensation processes. The resultant of nanoparticles was separated using a strong neodymium magnet and then dissolve in ethanol. The product termed as FePt@SiO₂.

Surface Modification of FePt@SiO₂ Using EDS Reaction

The *N*-[3-(trimethoxysilyl) propyl] ethylenediamine (EDS) was used for surface modification of FePt@SiO₂. Briefly, an equal volume of FePt@SiO₂ (183 mg/mL) and acetic acid were mixed with EDS under vigorously stirring for 1 h at room temperature which will resulted in amine-functionalized FePt@SiO₂ (FePt@SiO₂-N). The solution was subject to centrifugation at 4500 rpm for 30 min to

remove any traces. The resulting nanoparticles were collected using a strong neodymium magnet and then dissolve in deionized water. FePt@SiO₂-N with different concentration of EDS in the range of 0–0.5 M was prepared.

Preparation of Gold Nanoparticles

Gold nanoparticles were prepared through well-established citrate reduction techniques as method described previously with minor modification [30]. In a typical experiment, 103 mL of HAuCl₄ 0.33 mM was place on a three-neck round-bottom flask on a stirring hot plate. To the rapidly stirred boiling solution, 3.5 mL of a 1 % solution of trisodium citrate dihydrate (Na₃C₆H₅O₇·2H₂O) was quickly added. The gold sol gradually forms as the citrate reduces the gold (III). It was remove from heat when

the solution has turned deep red. The product was termed as gold nanoparticles (AuNPs).

Preparation of Au-FePt@SiO₂-N

Gold-surface modified FePt@SiO₂ was prepared through the simple mixing of gold solution and FePt@SiO₂-N. Briefly, FePt@SiO₂-N and Au NPs were mixed under vigorously stirring for 1 h at room temperature. The resulting nanoparticles were then centrifuged at 4500 rpm for 30 min to remove any traces and impurities. The resultant termed as gold nanoparticles-modified FePt@SiO₂-N (Au-FePt@SiO₂-N). Au-FePt@SiO₂-N with different Au concentration in the range of 0–238 μM was prepared.

Characterizations

Structure and morphology of the resultant nanoparticles were characterized by transmission electron microscopy using TEM-8100, Hitachi, at an acceleration voltage of 200 kV. Prior to the TEM observation, an aliquot of suspension of samples was diluted with water until optically clear. Briefly, an aliquot of suspension were placed on a carbon-coated Formvar copper grid (300 mesh, Electron Microscopy Sciences) to form a thin film specimen. The excess of the sample was blotted using a filter paper then air-dried overnight in a dust-free area before loading into the specimen chamber. Elemental analysis was performed using EDS analysis system attached to the same instrument. Zeta (ζ) potential was determined through electrophoretic mobility measurement and calculated using Helmholtz-Smoluchowski's equation. The zeta (ζ) potential of the samples were determined at 25 °C by using dynamic light scattering (DLS) spectrophotometer, Horiba Instrument, Horiba, Kyoto, Japan. All characterization measurements were repeated three times. The resultant of nanoparticles were further investigated using X-ray photoelectron spectroscopy (XPS) (ESCALAB 250, Thermo VG Scientific, West Sussex, UK) equipped with Mg K_α at 1253.6 eV at the anode to evaluate their chemical binding energy characteristics. Briefly, an aliquot of solution was put on silicon slice and dried overnight. Furthermore, the sample was then placed to XPS chamber and excited with X-rays with a monochromatic Al K_{α1,2} radiation. Magnetization as a function of the field was evaluated using a vibrating sample magnetometer (VSM) Lakeshore model 7400 at room temperature.

Bacteria Culture

S. aureus (ATCC 6538P) was used as the model of pathogenic bacteria. Briefly, frozen preserved stock was thawed at room temperature, and then 0.1 mL were pipetted and streaked into a quadrant on a nutrient agar plate. Nutrient agar was composed of 6 g Agar Bacteriological (Agar No. 1) LP0011 powder mixed with 10 g Difco™ LB Broth, Miller (Luria-Bertani) powder and

diluted with 400 mL deionized (DI) water and cultured at 37 °C for 18–24 h to allow the formation of colonies. Afterward, a single colony was scraped with a loop and swabbed onto a 15°-slant medium (nutrient agar) and then incubated at 37 °C for 18–24 h.

Surface-enhanced Raman Spectroscopy

Raman spectroscopy was conducted using Raman microscope instrument (HORIBA Jobin Yvon S.A.S.) equipped with laser ($\lambda = 633$ nm). The instrument was calibrated against a Si crystal. Prior to the experiment, an aliquot of Au-FePt@SiO₂-N solution was mixed equally with the concentrations of adenine (5×10^{-5} M) or *S. aureus* (5×10^6 CFU/mL) and then homogenized using vortex (VTX-3000 L Mixer Uzusio, LMS Co., Tokyo, Japan). Afterwards, the mixed suspension was dropped wisely into the alumina chip followed by drying in free dust-air atmosphere.

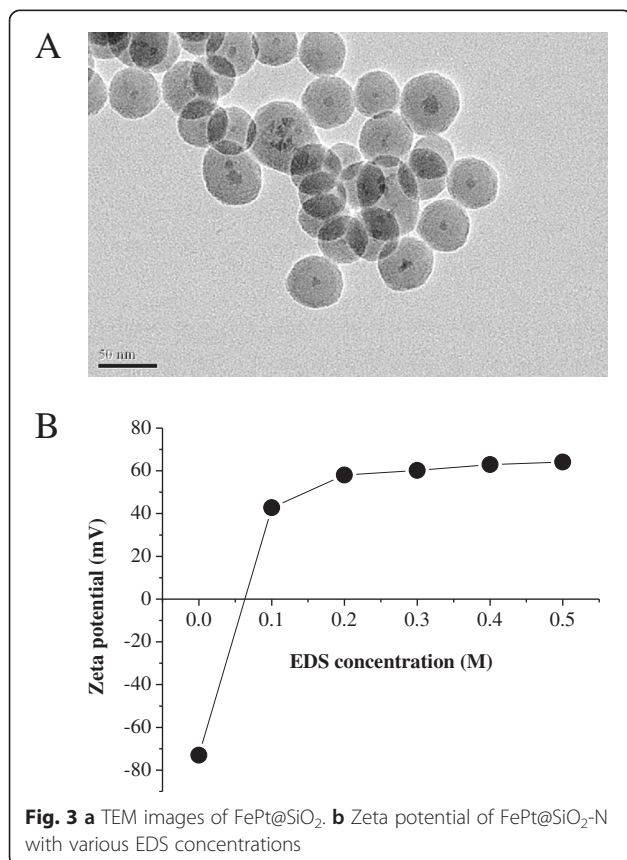
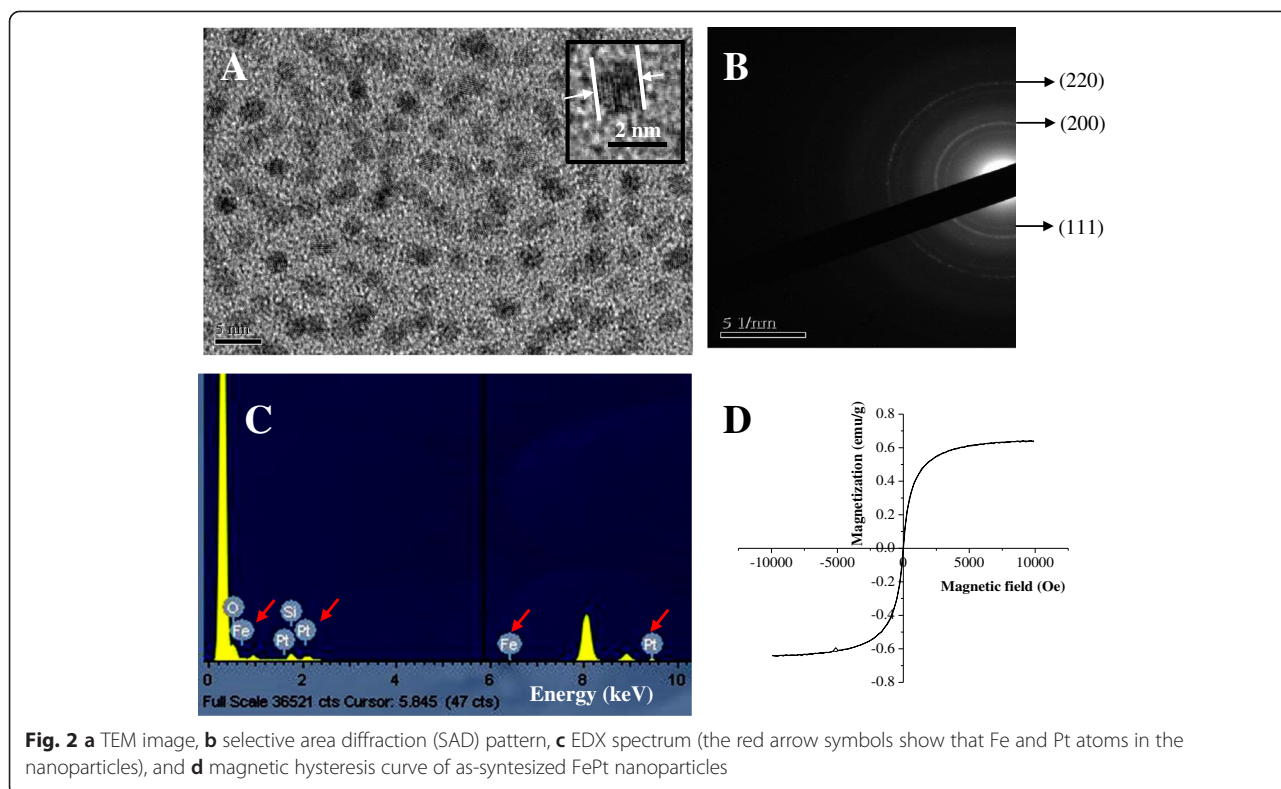
Results and Discussion

Structure and Morphology of FePt Nanoparticles

TEM images display homogeneously distribution of FePt nanoparticles, which are surface-protected by oleic acid and oleyl amine, and acted as ligands to stabilize FePt nanoparticles, as shown in Fig. 2a. Furthermore, oleic acid and oleic amine protecting the surface of FePt nanoparticles would further generate the hydrophobic characteristic of FePt nanoparticles [31]. The as-synthesized FePt nanoparticles could disperse homogeneously in the nonpolar solvents such as cyclohexane, due to the presence of oleic acid and oleylamine. The average diameter of the FePt nanoparticles was determined to be 2–3 nm. The insert of TEM image revealed the crystalline nature of FePt nanoparticles. The lattice fringes of the core are clearly shown in the image, corresponding to (111) lattice planes for FePt nanoparticles (Fig. 2b) [32]. Energy-dispersive X-ray spectroscopy (EDX) analysis shows that the particles contain the elements of Fe and Pt (Fig. 2c). VSM measurement revealed that FePt nanoparticles exhibited superparamagnetic characteristics with a single magnetic domain and exhibit magnetic moment in the presence of external magnetic field. When magnetic field is removed, the particles return to their nonmagnetic nature immediately (Fig. 2d).

Physicochemical Properties of FePt@SiO₂, FePt@SiO₂-N, and Gold Nanoparticles

Figure 3a shows the core-shell TEM images of FePt@SiO₂. It revealed the successful sol-gel reaction of the shell of silica (SiO₂) (25–30 nm) for encapsulation of the core of FePt nanoparticles. Most of the SiO₂ spheres encapsulated one FePt nanoparticle, and a small portion of the particles contains either zero or two FePt nanoparticles. The different



contrast between the core and shell region is due to the different electron penetration on metallic FePt nanoparticles and SiO₂ nanoparticle [32]. Moreover, FePt@SiO₂ nanoparticles could easily dispersed in water system. Surface modification of FePt@SiO₂ was developed through the reaction with *N*-[3-(trimethoxysilyl) propyl] ethylenediamine (EDS), called as FePt@SiO₂-N. The structure and morphology of FePt@SiO₂-N were also developed in the spherical structure (Additional file 1: Figure S1A). Figure 3b shows the zeta potential of amine-functionalized FePt@SiO₂ (FePt@SiO₂-N). Zeta potential measurement revealed that the surface charge of the FePt@SiO₂ nanoparticles, which would increase with the addition of EDS concentration increase, due to the positive charge (amine group) of EDS. After surface modification, the FePt@SiO₂-N nanoparticles are overall positively charged with the average zeta potential range from +40 until +60 mV Furthermore, we have successfully fabricate AuNPs through well-established citrate reduction method, and TEM images of gold nanoparticles revealed the spherical morphology in the diameter of ~17 nm (Additional file 1: Figure S1B).

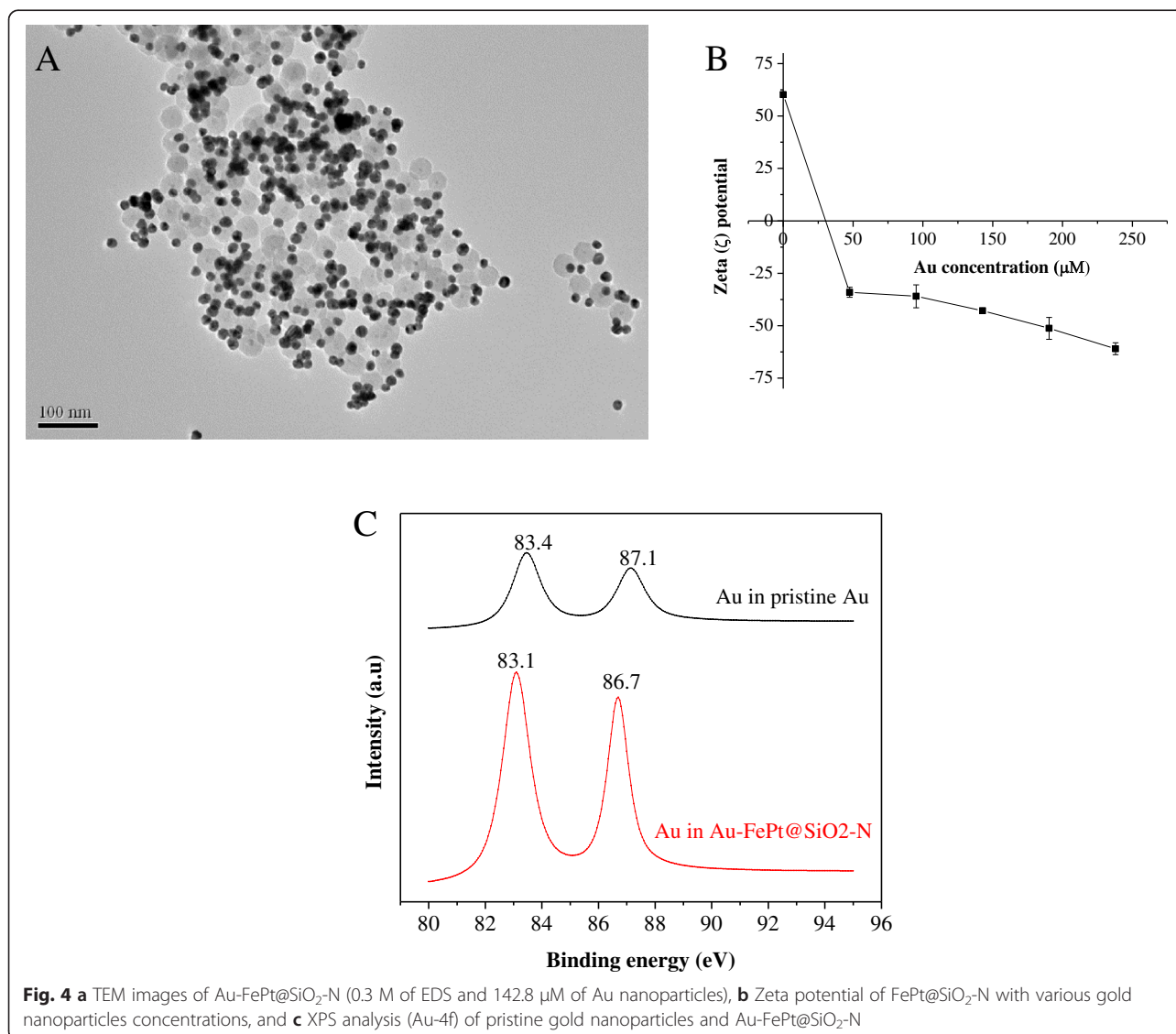
Structure and Morphology of Au-FePt@SiO₂-N

FePt@SiO₂-N could electrostatically attract negatively charged of Au nanoparticles (~17 nm) synthesized in advance by citrate reduction method of HAuCl₄ with

trisodium citrate dihydrate ($\text{Na}_3\text{C}_6\text{H}_5\text{O}_7 \cdot 2\text{H}_2\text{O}$). This result is in accordance with the previously reported research [19, 33]. As shown in Fig. 4a, TEM images of extensively washed Au-FePt@SiO₂-N nanoparticles revealed a dense surface coverage of gold nanoparticles. The attractive force between Au nanoparticles and FePt@SiO₂-N is sufficiently strong, which could tightly and stably attach each other, no matter how the FePt@SiO₂-N nanoparticles are centrifuged and re-dispersed by ultrasonication. Lower concentrations of EDS and gold nanoparticles exhibited a single nanoparticle attached on the FePt@SiO₂-N, where individual gold nanoparticles are homogeneously separated, as shown in SEM image (Additional file 1: Figures S2B, D and S3B, D). In contrast, higher concentration of EDS and gold nanoparticles show the clusters structure (Additional

file 1: Figures S2E, F and S3E, F). The optimum concentration of Au-FePt@SiO₂-N was found in 0.3 M of EDS and 142.8 μM of gold nanoparticles, which displays homogeneously distribution of Au nanoparticles.

Figure 4b shows the zeta potentials of Au-FePt@SiO₂-N with various gold concentrations. It revealed that the surface charged of the core-shell nanoparticles becomes negatively charged after gold immobilization by zeta potential measurement. This might be that the Au-trisodium citrate dihydrate nanoparticles coverage of FePt@SiO₂-N develops the net negatively charged nanoparticles, which further prove the successful immobilization of Au nanoparticles onto the surface of FePt@SiO₂-N. Figure 4c displays the region of the XPS spectra corresponding to Au-4f. Pristine gold nanoparticles exhibited binding energy of Au 4f_{7/2} and Au 4f_{5/2} at 83.4 and 87.1 eV,



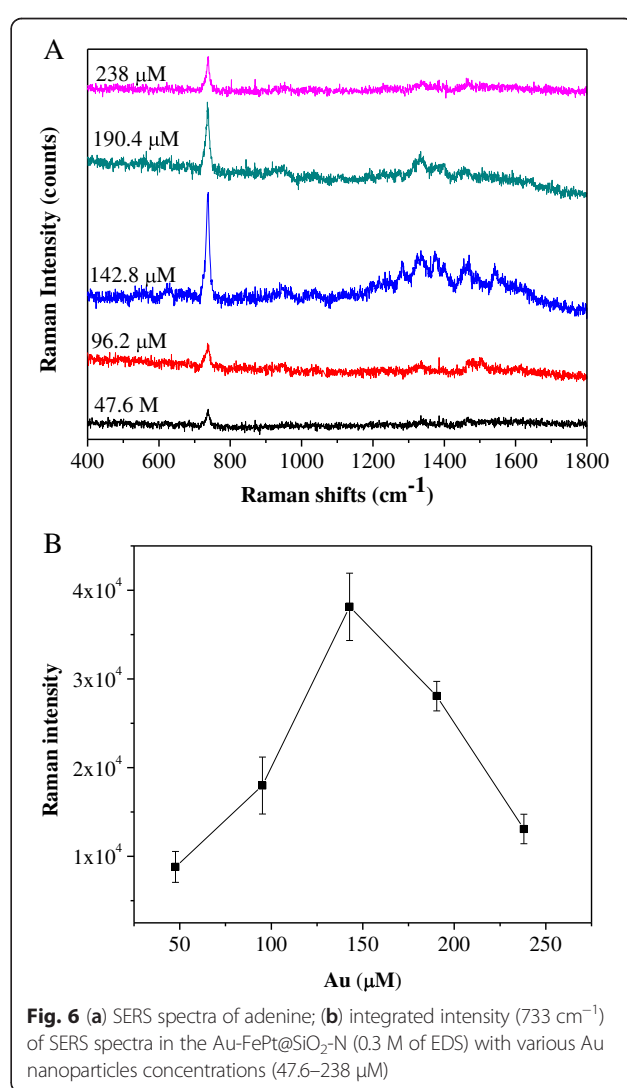
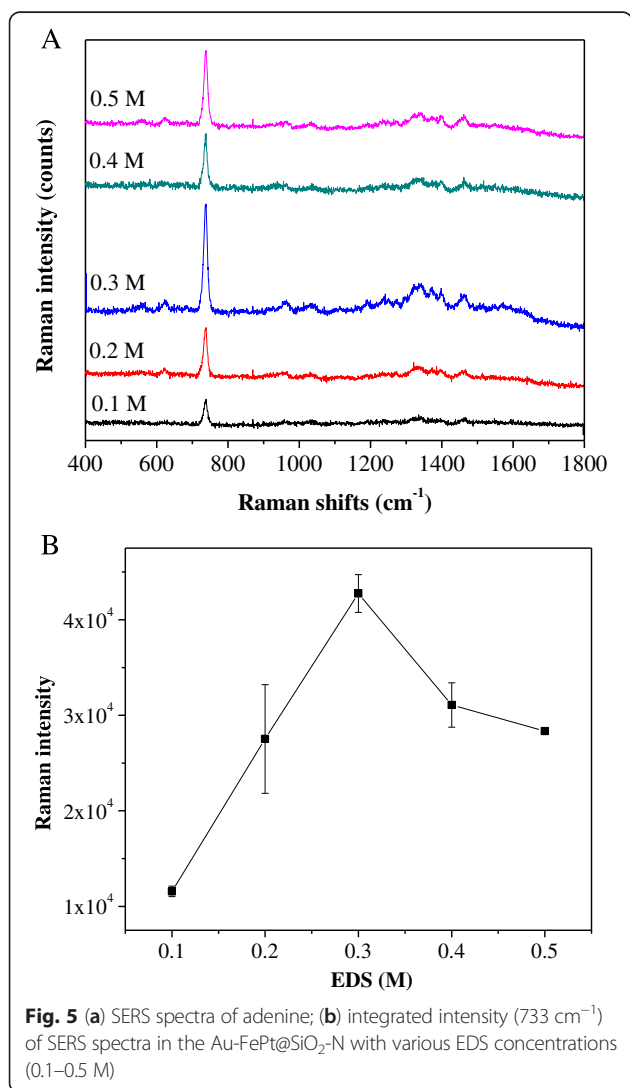
respectively. These peaks were shifted to 83.1 (Au-4f_{7/2}) and 86.7 eV (Au-4f_{5/2}) in the Au-FePt@SiO₂-N. The shifted peaks further confirmed the reaction between gold (Au) nanoparticles and FePt@SiO₂-N nanoparticles through electrostatic interaction.

SERS Detection of Adenine

The advantage to use the nanoparticle is its high-surface area could increase the interaction between adenine and the Au-FePt@SiO₂-N for surface-enhanced Raman scattering (SERS) bio-detection. Figure 5 shows the Raman spectrum of adenine in the various concentrations of Au-FePt@SiO₂-N with EDS concentration ranging from 0.1 to 0.5 M. Increasing EDS concentration of Au-FePt@SiO₂-N from 0 to 0.3 M will increase the Raman intensity (integrated peak at ~733 cm⁻¹) of adenine. The integrated peak at ~733 cm⁻¹ is assigned to the ring-breathing vibration of adenine [34]. However, Raman intensity slightly decreased at 0.4 and 0.5 M of EDS

concentration. This reason could be explained that EDS play an important role in the surface modification of FePt@SiO₂, which is further developed as a site for the reaction between the FePt@SiO₂ and gold nanoparticles (Au). This result is in agreement with the TEM results. At 0.3 M of EDS concentration, the gold nanoparticles could homogeneously disperse on the surface of FePt@SiO₂-N, thus, developed an optimum “hot spot” effect for Raman enhancement signals of adenine. High concentration of EDS could develop the high entrapment of gold nanoparticles become a gold clustering system. However, as the increasing of nanoparticles size and concentration, the convex shape of the surface becomes flatter, the particles could absorb less light and less inelastic scattering pronounce on the surface, which tend to weakening of electromagnetic field on the surface and the overall SERS intensity [35].

Figure 6 shows the Raman spectrum of adenine in various concentration of Au-FePt@SiO₂-N ranging from



47.6 to 238 μM . The optimum Raman enhancement signal was found in the 142.8 μM of Au-FePt@SiO₂-N. Raman signal of adenine slightly reduced at higher concentration of Au-FePt@SiO₂-N (190.4–238 μM). The result and mechanism are similar with the abovementioned EDS concentrations. The enhancement effect (EF) at 733 cm^{-1} of “adenine” on the Au-FePt@SiO₂-N SERS substrate are determined using the following expression: $\text{EF} = (I_{\text{SERS}}/N_{\text{SERS}})/(I_{\text{bulk}}/N_{\text{bulk}})$, where I_{SERS} is the intensity of a vibrational mode in the surface-enhanced spectrum, I_{bulk} is the intensity of the same mode in the Raman spectrum, N_{SERS} is the number of molecules adsorbed on the SERS substrate, and N_{bulk} is the number of molecules in the bulk. N_{SERS} can be obtained according to the method proposed by Orendorff et al. [36]. The enhancement factor of Au-FePt@SiO₂-N (0.3 M of EDS and 142.8 μM of gold nanoparticles) is about 2×10^7 magnification.

SERS Detection of Bacteria (*S. aureus*)

There is currently increasing significant development of SERS nanotechnology for the rapid characterization and identification of bacteria. SERS nanotechnology could observe the chemical molecular components of the bacteria cell walls and provide the chemical identification of bacteria for clinical diagnostics. In this respect, the surface characteristics and the affinity between samples and SERS nano hybrids are important, which would affect the detected limitation of SERS signals and the intensities of the SERS spectra. Thus, if the bacterial cell walls can effectively been attached to the surface of SERS nano hybrids, it will contribute to highly enhanced Raman signal [4, 23]. Vibrational bands of nucleic acids, proteins, phospholipids, and polysaccharides are anticipated to contribute to the Raman spectra. For example, the strong bacterial SERS band at $\sim 735 \text{ cm}^{-1}$ has been attributed to the nucleic acid base adenosine [24, 37]. The SERS spectra for *S. aureus* (0.5×10^7 CFU/mL) assays observed by using Au-FePt@SiO₂-N with various gold nanoparticles concentration are shown in Fig. 7, which displays a typical SERS response after the incubation with *S. aureus*. The spectra contain features which are attributable to SERS of *S. aureus* and are dominated by bands that are representative of the bacteria membrane protein. The outer bacteria cell layer sensitivity of this spectroscopic method makes the assignment of this band and features at 965, 1030, and 1080 cm^{-1} more likely developed from the lipid layer components of the cell walls and membranes. Raman signal at 715 cm^{-1} (C-N stretching) and 1060 cm^{-1} (C-C stretching) are well-known markers of lipid layer fluidity, and vibrational bands in the 930–1130 cm^{-1} region have been also previously assigned to membrane phospholipids. Amide I, II, and III vibrations, associated with protein backbone, and

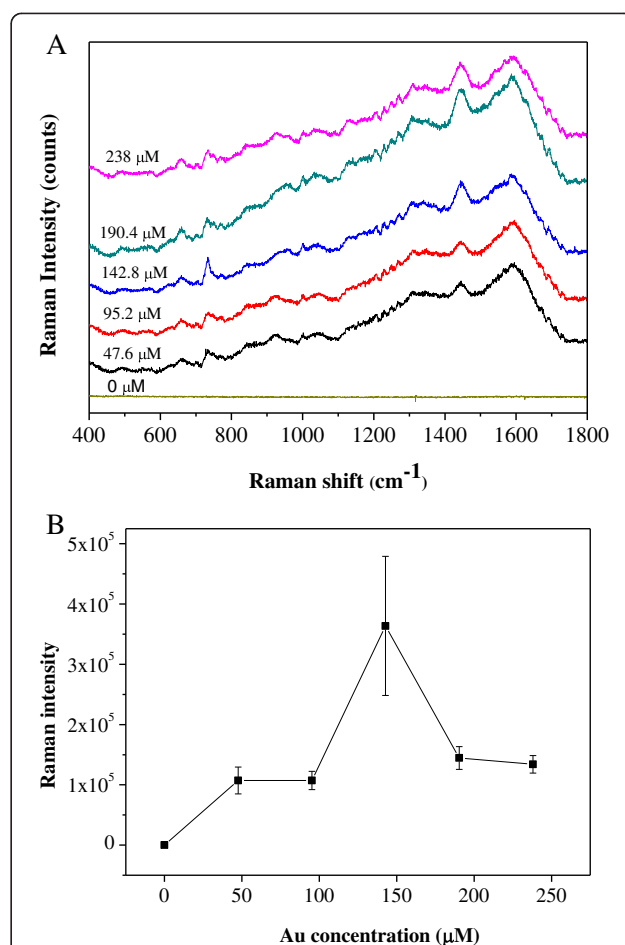
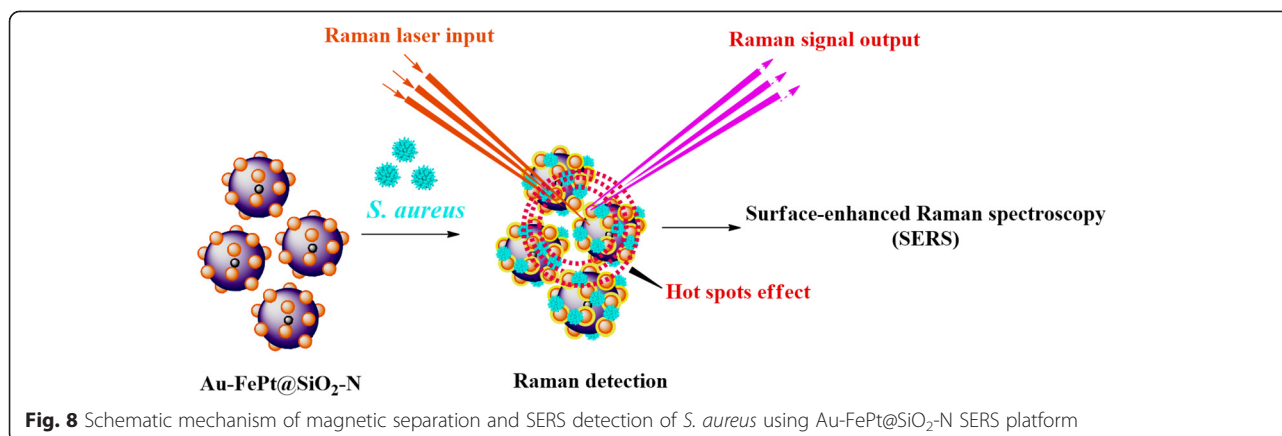


Fig. 7 (a) SERS spectra of *S. aureus*; (b) integrated intensity (735 cm^{-1}) of SERS spectra in the Au-FePt@SiO₂-N (0.3 M of EDS) with various Au nanoparticles concentrations (47.6–238 μM)

carboxylic stretches, are expected in the 1310–1589 cm^{-1} region and probably dominate the SERS vibrational signature in this region [24]. As shown in Fig. 7, the optimum enhancement of SERS signals could be reached using 142.8 μM gold nanoparticles in Au-FePt@SiO₂-N. This might be due to the increasing gold concentration that could increase the surface area of the nanoparticles then provide the larger sites for bacteria entrapment thus increasing the Raman signal of *S. aureus*, and also it might be due to the development an appropriate hot spot effect for enhancement of Raman signal. This is in accordance with previously reported researches [2, 38]. Raman signal of *S. aureus* slightly reduced at higher concentration of Au-FePt@SiO₂-N (190.4–238 μM) which is similar with the result of detecting adenine in Fig. 6.

Conclusions

We fabricated multifunctional core-shell nanostructures of gold nanoparticles-decorated silica encapsulated FePt



(Au-FePt@SiO₂-N), which could be developed in the SERS detection, such as small biomolecules (adenine) and pathogenic bacteria (*S. aureus*). SERS spectra of adenine and *S. aureus* obtained from the Au-FePt@SiO₂-N core-shell nanoparticles showed finger-print peaks with significant enhancement on the Raman signal. Furthermore, the magnetic core of FePt nanoparticles could be applied in the rapid magnetic separation of the biomolecules and bacteria and achieve the condensed effect. Therefore, the novel SERS platform of core-shell structure of Au-FePt@SiO₂ nanoparticles (Fig. 8) would provide the potential to apply in the magnetic separation and bio-sensing at the same time, which could save the diagnosis time significantly.

Additional file

Additional file 1: TEM images of core-shell nanoparticles. Figure S1.

TEM images of (A) FePt@SiO₂-N and (B) gold nanoparticles (scale bar: 50 nm). **Figure S2.** TEM images of Au-FePt@SiO₂-N with various EDS concentration: (A) 0 mM, (B) 0.1 M, (C) 0.2 M, (D) 0.3 M, (E) 0.4 M and (F) 0.5 M (scale bar: 50 nm). **Figure S3.** TEM images of Au-FePt@SiO₂-N (0.3 M) with various gold concentration: (A) 0 μM, (B) 47.6 μM, (C) 95.2 μM, (D) 142.8 μM, (E) 190.4 μM, and (F) 238 μM (scale bar, 100 nm)

Competing interests

The authors declare that they have no competing interests.

Authors' contributions

AH, AYC, MCY, CYK, and TYL had conceived and designed the experiments. AH, AYC, HLL, TYC, and HMT performed the experiments. TYL, CYK, JKW, and YLW contributed ideas and material analyses. AH, AYC, TYL and MCY wrote the manuscript. All authors read and approved the final manuscript.

Authors' information

AH is a PhD student at National Taiwan University of Science and Technology. AYC and HLL are graduate students from National Taiwan University of Science and Technology. MCY holds a professor position at the National Taiwan University of Science and Technology. TYL holds an assistant professor position at Ming Chi the University of Technology. TYC and HMT are undergraduate students at the Ming Chi University of Technology. CYK is a PhD student at National Taiwan University. JKW is a researcher at National Taiwan University and Academia Sinica, Taiwan. YLW is a researcher at Academia Sinica, Taiwan, and a professor at National Taiwan University.

Acknowledgements

This work was financially supported by the Ministry of Science and Technology of Taiwan (MOST 104-2221-E-131-010 and MOST 104-2628-M-001-009) and partially supported by the Academia Sinica. Technical support of VSM from Nano group Public Laboratory, Institute of Physics, at Academia Sinica in Taiwan, is acknowledged.

Author details

¹Department of Materials Science and Engineering, National Taiwan University of Science and Technology, Taipei 10607, Taiwan. ²Department of Materials Engineering, Ming Chi University of Technology, New Taipei City 24301, Taiwan. ³Institute of Polymer Science and Engineering, National Taiwan University, Taipei 10617, Taiwan. ⁴Center for Condensed Matter Sciences, National Taiwan University, Taipei 10617, Taiwan. ⁵Institute of Atomic and Molecular Sciences, Academia Sinica, Taipei 10617, Taiwan. ⁶Department of Physics, National Taiwan University, Taipei 10617, Taiwan.

Received: 24 August 2015 Accepted: 8 October 2015

Published online: 22 October 2015

References

- Syed MA, Bokhari SH (2011) Gold nanoparticle based microbial detection and identification. *J Biomed Nanotechnol* 7:229–237
- Lin C-C, Yang Y-M, Liao P-H, Chen D-W, Lin H-P, Chang H-C (2014) A filter-like AuNPs@MS SERS substrate for Staphylococcus aureus detection. *Biosens Bioelectron* 53:519–527
- Liu T-T, Lin Y-H, Hung C-S, Liu T-J, Chen Y, Huang Y-C, Tsai T-H, Wang H-H, Wang D-W, Wang J-K, Wang Y-L, Lin C-H (2009) A high speed detection platform based on surface-enhanced raman scattering for monitoring antibiotic-induced chemical changes in bacteria cell wall. *PLoS One* 4, e5470
- Wang H, Zhou Y, Jiang X, Sun B, Zhu Y, Wang H, Su Y, He Y (2015) Simultaneous capture, detection, and inactivation of bacteria as enabled by a surface-enhanced raman scattering multifunctional chip. *Angew Chem Int Ed* 54:5132–5136
- Liu T-Y, Chen Y, Wang H-H, Huang Y-L, Chao Y-C, Tsai K-T, Cheng W-C, Chuang C-Y, Tsai Y-H, Huang C-Y, Wang D-W, Lin C-H, Wang J-K, Wang Y-L (2012) Differentiation of bacteria cell wall using Raman scattering enhanced by nanoparticle array. *J Nanosci Nanotechnol* 12:5004–5008
- Yang H, Deng M, Ga S, Chen S, Kang L, Wang J, Xin W, Zhang T, You Z, An Y, Wang J, Cui D (2014) Capillary-driven surface-enhanced Raman scattering (SERS)-based microfluidic chip for abrin detection. *Nanoscale Res Lett* 9:138
- Cottat M, Lidgi-Guigui N, Tijunelyte I, Barbillon G, Hamouda F, Gogol P, Aassime A, Lourtioz JM, Bartenlian B, de la Chapelle ML (2014) Soft UV nanoimprint lithography-designed highly sensitive substrates for SERS detection. *Nanoscale Res Lett* 9:2361
- Kennedy BJ, Spaeth S, Dickey M, Carron KT (1999) Determination of the distance dependence and experimental effects for modified SERS substrates based on self-assembled monolayers formed using alkanethiols. *J Phys Chem B* 103:3640–3646

9. Nie S, Emory SR (1997) Probing single molecules and single nanoparticles by surface-enhanced raman scattering. *Science* 275:1102–1106
10. Haynes CL, Van Duyne RP (2003) Plasmon-sampled surface-enhanced raman excitation spectroscopy. *J Phys Chem B* 107:7426–7433
11. Kelly KL, Coronado E, Zhao LL, Schatz GC (2003) The optical properties of metal nanoparticles: the influence of size, shape, and dielectric environment. *J Phys Chem B* 107:668–677
12. Culha M, Cullum B, Lavrik N, Klutse CK (2012) Surface-enhanced raman scattering as an emerging characterization and detection technique. *J Nanotechnology* 2012:15
13. Drake P, Jiang P-S, Chang H-W, Su S-C, Tanha J, Tay L-L, Chen P, Lin Y-J (2013) Raman based detection of *Staphylococcus aureus* utilizing single domain antibody coated nanoparticle labels and magnetic trapping. *Anal Methods* 5:4152–4158
14. Liu M, Wang Z, Zong S, Zhang R, Zhu D, Xu S, Wang C, Cui Y (2013) SERS-based DNA detection in aqueous solutions using oligonucleotide-modified Ag nanoprisms and gold nanoparticles. *Anal Bioanal Chem* 405:6131–6136
15. Tian F, Bonnier F, Casey A, Shanahan AE, Byrne HJ (2014) Surface enhanced Raman scattering with gold nanoparticles: effect of particle shape. *Anal Methods* 6:9116–9123
16. Herrera G, Padilla A, Hernandez-Rivera S (2013) Surface enhanced Raman scattering (SERS) studies of gold and silver nanoparticles prepared by laser ablation. *Nanomaterials* 3:158
17. Jarvis RM, Goodacre R (2004) Discrimination of bacteria using surface-enhanced Raman spectroscopy. *Anal Chem* 76:40–47
18. Cheng IF, Chen TY, Lu RJ, Wu HW (2014) Rapid identification of bacteria utilizing amplified dielectrophoretic force-assisted nanoparticle-induced surface-enhanced Raman spectroscopy. *Nanoscale Res Lett* 9:324
19. Westcott SL, Oldenburg SJ, Lee TR, Halas NJ (1998) Formation and adsorption of clusters of gold nanoparticles onto functionalized silica nanoparticle surfaces. *Langmuir* 14:5396–5401
20. Yeh Y-C, Creran B, Rotello VM (2012) Gold nanoparticles: preparation, properties, and applications in bionanotechnology. *Nanoscale* 4:1871–1880
21. Zhou J, Ralston J, Sedev R, Beattie DA (2009) Functionalized gold nanoparticles: synthesis, structure and colloid stability. *J Colloid Interface Sci* 331:251–262
22. Zhang Y, Chu W, Foroushani A, Wang H, Li D, Liu J, Barrow C, Wang X, Yang W (2014) New gold nanostructures for sensor applications: a review. *Materials* 7:5169
23. Yan B, Thubagere A, Premasiri WR, Ziegler LD, Dal Negro L, Reinhard BM (2009) Engineered SERS substrates with multiscale signal enhancement: nanoparticle cluster arrays. *ACS Nano* 3:1190–1202
24. Premasiri WR, Moir DT, Klempner MS, Krieger N, Jones G, Ziegler LD (2005) Characterization of the surface enhanced raman scattering (SERS) of bacteria. *J Phys Chem B* 109:312–320
25. Saverot SE, Reese LM, Cimini D, Vikesland PJ, Bickford LR (2015) Characterization of conventional one-step sodium thiosulfate facilitated gold nanoparticle synthesis. *Nanoscale Res Lett* 10:940
26. Yigit MV, Medarova Z (2012) In vivo and ex vivo applications of gold nanoparticles for biomedical SERS imaging. *Am J Nucl Med Mol Imaging* 2:232–241
27. Bishnoi SW, Lin Y-j, Tibudan M, Huang Y, Nakaema M, Swarup V, Keiderling TA (2011) SERS biodetection using gold–silica nanoshells and nitrocellulose membranes. *Anal Chem* 83:4053–4060
28. Kim N, Son S-H (2015) Development of antigen-immobilized metallothionein sensor that exploits gold nanoparticle-based enhancement of signal. *J Nanosci Nanotechnol* 15:6188–6192
29. Tamer U, Cetin D, Suludere Z, Boyaci IH, Temiz HT, Yegenoglu H, Daniel P, Dinçer İ, Elerman Y (2013) Gold-coated iron composite nanospheres targeted the detection of *Escherichia coli*. *Int J Mol Sci* 14:6223–6240
30. Ojea-Jiménez I, Romero FM, Bastús NG, Puentes V (2010) Small gold nanoparticles synthesized with sodium citrate and heavy water: insights into the reaction mechanism. *J Phys Chem C* 114:1800–1804
31. Mori K, Yamashita H (2010) Progress in design and architecture of metal nanoparticles for catalytic applications. *Phys Chem Chem Phys* 12:14420–14432
32. Aslam M, Fu L, Li S, Dravid VP (2005) Silica encapsulation and magnetic properties of FePt nanoparticles. *J Colloid Interface Sci* 290:444–449
33. Stoeva SI, Huo F, Lee J-S, Mirkin CA (2005) Three-layer composite magnetic nanoparticle probes for DNA. *J Am Chem Soc* 127:15362–15363
34. Gearheart LA, Ploehn HJ, Murphy CJ (2001) Oligonucleotide adsorption to gold nanoparticles: a surface-enhanced raman spectroscopy study of intrinsically bent DNA. *J Phys Chem B* 105:12609–12615
35. Hong S, Li X (2013) Optimal size of gold nanoparticles for surface-enhanced Raman spectroscopy under different conditions. *J Nanomater* 2013:9
36. Orendorff CJ, Gearheart L, Jana NR, Murphy CJ (2006) Aspect ratio dependence on surface enhanced Raman scattering using silver and gold nanorod substrates. *Phys Chem Chem Phys* 8:165–170
37. Chu H, Huang Y, Zhao Y (2008) Silver nanorod arrays as a surface-enhanced Raman scattering substrate for foodborne pathogenic bacteria detection. *Appl Spectrosc* 62:922–931
38. Lin C-C, Chang C-W (2014) AuNPs@mesoSiO₂ composites for SERS detection of DTNB molecule. *Biosens Bioelectron* 51:297–303

Submit your manuscript to a SpringerOpen® journal and benefit from:

- Convenient online submission
- Rigorous peer review
- Immediate publication on acceptance
- Open access: articles freely available online
- High visibility within the field
- Retaining the copyright to your article

Submit your next manuscript at ► springeropen.com
